Effect of the thickness of thallium deposits on the values of EQCM sensitivity constant

Ana-Laura Donjuan-Medrano and Antonio Montes-Rojas*

Received (in Montpellier, France) 28th May 2008, Accepted 18th June 2008
First published as an Advance Article on the web 21st August 2008
DOI: 10.1039/b808802k

Three methods were used to obtain values of the sensitivity constant (C_f) of an electrochemical quartz crystal microbalance (EQCM) using solutions of Tl^+ ions: chronoamperometry, chronopotentiometry and cyclic voltammetry. The results obtained by these three methods showed that the C_f values were very sensitive to experimental conditions used to form deposits and the three techniques revealed that C_f is markedly influenced by the roughness of thallium films. For example, if the thickness is low or too high, the relative error of C_f with respect to the theoretical value is in the order of −20% due to its roughness and mechanical stress produced by the difference in atomic size. On the contrary, if the thicknesses are intermediate, the C_f values approach the theoretical value with errors that may be below +5%. Furthermore, the electrodes employed in this determination can be used again without important modifications in their surface composition.

1. Introduction

The electrochemical quartz crystal microbalance (EQCM) results from coupling microgravimetry which uses a quartz crystal microbalance (QCM) to classical electrochemical techniques, such as voltammetry, chronoamperometry or more recently, electrochemical impedance and forced convection techniques.[1–5] EQCM has been broadly used in past years in different studies to obtain information on some processes occurring at the electrochemical interface, such as growth of metallic[6,7] or non-metallic films,[8,9] adsorption of ionic[10–12] or neutral species,[13,14] *etc*. This technique is based on the principle that has been widely explained in the literature and the authors of this paper recommend reviewing the excellent works of Buttry and Ward[15] or Hepel[16] for further information. Herein, we will only mention that when a sheet of an acentric material, such as quartz, covered by a thin metal layer on both sides, is placed in an electric field whose polarity changes periodically, an acoustic wave develops and displaces perpendicularly through the surface of this sheet (resonator) characterized by a resonance frequency (f_o). If for any reason, a material is deposited on one of the sides of this sheet, the resonance frequency will change to a new value giving rise to a variation of frequency ($\Delta f(m) = f - f_o$) proportional to the change of mass. In electrochemistry, one side of the resonator may be used as electrode, which allow the total frequency variation, Δf, to include in addition to the mass variations, also other contributions considered in the expression

$$\Delta f = \Delta f(T) + \Delta f(P) + \Delta f(r) + \Delta f(v) + \Delta f(m) \qquad (1)$$

where $\Delta f(T)$ is the frequency variation associated with the changes of temperature, $\Delta f(P)$ is the frequency variation associated with the pressure changes, $\Delta f(r)$ is the frequency variation due to the changes of roughness, and $\Delta f(v)$ is the frequency variation caused by the changes in viscosity at the electrochemical interface.

However, these terms may be made irrelevant with respect to the value of $\Delta f(m)$, so that the total frequency variation is equal to frequency variations resulting from mass changes only produced on the resonator. It is just in this situation that Sauerbrey expression may be considered[17] (eqn (2)) in order to obtain information from experiments made with EQCM.

$$\Delta f(m) = -(f_0^2/N\rho_q)\Delta m \qquad (2)$$

In this equation Δm is the change of mass per area unit (g cm^{-2}), ρ_q is the quartz density (2.648 g cm^{-3}) and N is the frequency constant of the quartz (1.67×10^5 Hz cm^{-1}). The expression (2) may be simplified if the constants appearing between parentheses are grouped into a single constant, C_f (g^{-1} Hz cm^2), denoted as the sensitivity constant:

$$C_f = f_0^2/N\rho_q \qquad (3)$$

According to the main consideration posed by Sauerbrey to obtain his expression, the generated acoustic wave displaces in the same way in quartz as in the deposited material; therefore this latter may be considered as the quartz sheet grows in such a way that the mass variation of the deposited material must be equivalent to frequency variations below 2%[18] of the fundamental frequency. Furthermore, the deposited material must meet other characteristics for this assumption to be valid, for example, to be uniformly distributed all over the active area of the resonator as well as to be rigidly linked.

As C_f considers parameters depending upon the nature and design of the quartz sheet that not always behave ideally, this term must be determined quickly and precisely for each

Laboratorio de Electroquímica, Centro de Investigación y Estudios de Posgrado, Facultad de Ciencias Químicas, Universidad Autónoma de San Luis Potosí, Av. Dr Manuel Nava No. 6, Zona Universitaria, SLP, 78210, SLP México. E-mail: antonio.montes@uaslp.mx; Fax: (0052) 48262371; Tel: (0052) 48262372

resonator if quantitative information is to be obtained from this technique. There are numerous publications in the literature reporting some procedures to determine the value of C_f by using a calibration process. According to these publications, the value of C_f can be determined by the formation of a metallic deposit obtained potentiostatically,[19] galvanostatically[20] or by using voltammetry.[21] Silver[19] and copper[20] are some of the most commonly used metals for obtaining C_f[22,23] although other metals and procedures have been proposed to this purpose.

As far as copper is concerned[19] the galvanostatically obtained values of C_f are far from the expected value with errors ranging from 1% up to 12% when the thickness increases from 0 to 125 kHz. This is due to the fact that Cu^{2+} ion reduction is not through the direct reaction

$$Cu^{2+} + 2e \rightarrow Cu \quad (4)$$

but rather through reactions

$$Cu^{2+} + e \rightarrow Cu^{+} \quad (5)$$

$$Cu^{+} + e \rightarrow Cu \quad (6)$$

in which intermediate Cu^{+} species is produced, stable in the presence of complexing species.[24,25] In addition, this deviation has also been associated with the fact that copper deposition onto gold exhibits high roughness which causes an important interaction of the copper deposit with the adjacent liquid medium,[26] for which reason the Sauerbrey equation does not apply. Another important factor to consider is that during initial stages of the formation of these Cu deposits onto Au, an internal tension develops in these films due to the difference in atomic sizes between Cu and Au substrate, which may give rise to many monolayers of the deposit. Lastly, another, even greater inconvenience of the use of this metal for determining C_f is that the formation of a copper deposit onto a metal substrate such as Au or Pt is produced concurrently not only with the abundant formation of hydrogen, but also with the possible formation of surface alloys with the substrate,[27,28] causing their uselessness in further experiments.

The determination of C_f using Ag is simpler because the deposit formation takes place in a single stage without formation of intermediates

$$Ag^{+} + e \rightarrow Ag \quad (7)$$

In addition, the galvanostatically formed films[19] are smoother maintaining the validity of eqn (2). On the other hand, errors relative to the expected value are lower than those obtained using copper, since they may range between 1 and 5% when the silver film thickness is between 0 and 15 kHz. Despite this information, the values of the constant depend on the method used to obtain it, because the relative errors range from 5%, when it is obtained at constant current,[19] through 9% when potentiostatic method is used,[19] up to 25% when it is obtained by voltammetry.[21] Furthermore, as in the case of copper, the proven formation of surface alloys with Au and Pt[29,30] and the abundant formation of hydrogen does not allow the re-use of these resonators for further experiments.

On the other hand, more recently, Ratieuville *et al.*[31] determined C_f values by chronoamperometry using a solution of $AgNO_3$ with Pt and Au resonators. They found that the electrodeposition of silver on a gold electrode seems to be more accurate than that obtained on platinum because it has better electrochemical activation on gold than on platinum. The values found differ by less than 1% with respect to the theoretical value.

Some authors[22,23] have suggested other metals to determine C_f, *e.g.*, the use of thallium or lead which do not have the inconvenience referred to above, *i.e.* they are not obscured by hydrogen evolution if the pH is greater than 3.5 or 4.5, respectively, and the reduction of Pb(II) to Pb metal produces no stable Pb(I) species, so the reaction proceeds with 100% current efficiency. Likewise, the re-dissolution of bulk lead upon reverse voltammetric scan occurs with 100% current efficiency (no passivating oxide is formed), which means that the electrode surface can readily be restored to its original condition by voltammetric cycling.[32] However, for some authors it is clear that the Pb deposit on the gold can form surface alloys[33] when the potential applied is more negative than the thermodynamic potential. In the case of thallium,[23,34] its deposits on different substrates are known to exhibit similar reversible behavior, at least on carbon, gold, platinum and silver. Additionally, this metal is also known not to form alloys with gold or platinum electrodes, so such electrodes, used in the determination of C_f can be reused without any changes in their original condition.

It is important to mention that in most work reported on this issue, the effect of the metal film thickness on the value of sensitivity constant is only marginally referred to. So, the present work shows results of the C_f determination on gold resonators using films of Tl at different thicknesses obtained by three electrochemical methods.

2. Experimental

2.1 Reagents and solutions

All reagents (Tl_2CO_3, $NaClO_4$, H_2SO_4 *etc.*) were analytical grade and used as received. Water used in solution preparation was purified in a Millipore system (>18 MΩ cm).

Experimental condition solutions were selected using the Pourbaix's diagram of Tl in a medium with the absence of complex species.[35]

In accord with this diagram, only the hydrated metallic ion exists in a large pH range (pH −2 to 6), and the reaction of thallium in this pH range is

$$Tl^{+} + e \leftrightarrows Tl \quad (8)$$

In agreement with this diagram, at pH values between −2 and 2, reaction (9) is promoted thermodynamically

$$2H^{+} + 2e \leftrightarrows H_2\uparrow \quad (9)$$

so the formation of H_2 can take place concomitantly with the reduction by the Tl^{+} ion.

Therefore, the solution to use in this work must meet two minimum conditions:

(a) Not to have complex species in the bulk, and

(b) to have a pH value less acidic than 2, in order to eliminate reaction (9) as much as possible.

To this purpose, a solution of 1 M $NaClO_4$ was used as supporting electrolyte and a pH value 3.5 was selected using $HClO_4$. The thallium ion concentration was 1 or 5 mM.

Finally, prior to each experiment the solution was deaerated with high purity nitrogen and measurements were performed between three and five times by each of the three methods.

2.2 Electrodes

Planar AT-cut quartz crystals (Seiko) having a resonant frequency of ~9 MHz in air were used as the working electrodes in all experiments. The Au working electrode used in the EQCM was scanned in 0.1 M H_2SO_4 or $HClO_4$ solutions until a stable and standard cyclic voltammogram (CV) was obtained. The Au surface roughness factor, $R = 1.12$, was determined through charge density associated with an AuO monolayer subtracted by the double-layer charge.

A platinum sheet was used as the counter electrode, and an Ag|AgCl (3 M KCl) electrode as the reference electrode, against which all potentials were measured and reported.

2.2 Apparatus

Electrochemical experiments were carried out using an EG&G potentiostat–galvanostat model 273 A coupled to a QCM EG&G-Seiko model 910.

2.3 Experimental methodology

2.3.1. Treatment of electrodes. Each new Au electrode was previously cycled 100 times between 0.5 and 1.4 V in a solution of $HClO_4$ 0.1 M at 400 mV s^{-1} in order to release any stress from the near-surface region. The quality of the Au layer and its cleanliness were verified by recording CV profiles over the range −0.25 to −1.5 V in 0.1 M H_2SO_4.

2.3.2. Cyclic voltammetric measurements. Voltammetric measurements were performed in a potential range of +450 to −1100 mV at a scan rate between 5 and 50 mV s^{-1}.

2.3.3. Potentiostatic measurements. The potentiostatic measurements (chronoamperometric) were carried out by applying potential steps from an initial potential (E_i) to different final potentials (E_f); the duration (Δt) of the step was 120 s. Prior to the chronoamperometric measurements, CV and frequency responses were determined in metallic solution at a potential of 5 mV s^{-1} with the aim of choosing the potential region of E_i and E_f.

2.3.4. Galvanostatic measurements. The current used for galvanostatic experiments was selected between 98 and 80% of the limiting current (I_{lim}). The limiting current value was obtained by extrapolation at zero scan rate of the I_{lim} *vs.* scan rate curve using cyclic voltammetry.

It is important to mention that all experiments were carried out without stirring the solution.

2.3.5. Checking of the electrodes after measurements. Finally, a CV of the substrate was recorded after the calibration process in 0.1 M H_2SO_4 aimed at verifying whether the substrate surface was restored to its original condition.

2.3.6. Determination of C_f values. The electrochemical reaction involved in the electrodeposition of thallium can be represented by

$$M^{n+} + ne \rightarrow M \quad (8')$$

Using Faraday's second law:

$$\Delta Q = (nF/M_r)\Delta M \quad (10)$$

where ΔQ (C cm^{-2}) is the charge density measured from the electrochemical response; ΔM (g cm^{-2}) corresponds to the mass change of thallium on the Au electrode during electrodeposition process; n is the number of electrons transferred in the electrodeposition reaction (in the case of Tl deposition $n = 1$); M_r (g mol^{-1}) is the molar mass of M, and F (C mol^{-1}) is the Faraday constant.

By combining the Sauerbrey's equation (eqn (2)) with the above formula, we obtain the following relation that is used in the experimental determination of the calibration constant for the EQCM:

$$\Delta f = (C_f M_r/nF)\Delta Q \quad (11)$$

In consequence, the determination of C_f values consists in preparing curves of ΔQ as a function of Δf, where ΔQ is generated from the electrochemical responses obtained in each experimental method.

3. Results and discussion

3.1 Gold substrates

Fig. 1 shows a typical voltammetric response (CV) of an Au electrode used in this work in a sulfuric acid solution.

In this figure, two potential zones can be seen.

Zone I: Here, the CV is characterized by a very small and constant current. This behavior of CV is typical of the process of electrochemical interface charging. In addition, there are no Faradaic processes in this section of CV, which is a proof of cleanliness of our electrodes.

Zone II: We clearly detect both cathodic and anodic current peaks. These peaks are associated with Faradaic processes of formation/destruction of gold oxides.[36]

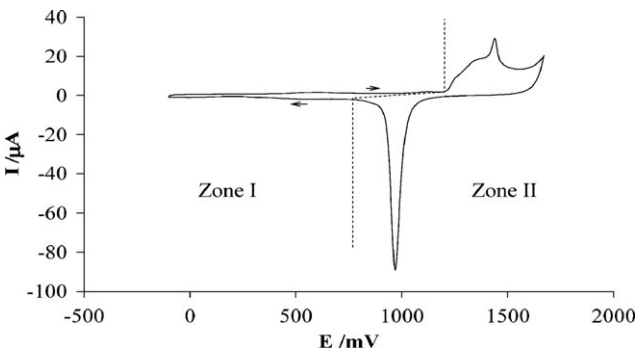

Fig. 1 A typical voltammetric response (CV) of an Au electrode used in this work obtained in 0.1 M H_2SO_4at 50 mV s^{-1}; geometrical area = 0.1965 cm^2.

3.2. Sensitivity constant with Tl

3.2.1 Voltammetric method. Cyclic voltammetry experiments were performed at different scan rates of 5, 10, 25 and 50 mV s^{-1} using a potential window which included the reversible potential of thallium (E_r = −739 mV) whose corresponding changes in frequency responses were recorded.

Fig. 2 shows a family of different CVs (Fig. 2(a)) and the corresponding frequency responses (Fig. 2(b)) for thallium deposition on and stripping from the Au electrode surface obtained from the Tl^+ solution in 1 M $NaClO_4$ (pH 3.5). When the potential is scanned between +400 and −550 mV, the current obtained is very low, but there are two current peaks at −100 mV associated with underpotential deposition (UPD) of thallium on gold substrate[37,38] which are not visible in our responses. It is noteworthy that during this process, thallium forms a monolayer on the gold substrate which tends to compact as the potential approaches the reversible potential, E_r.[38] On other hand, as the potential is swept from −500 mV towards more negative values, the response obtained shows a current cathodic peak between −729 and −745 mV. This peak is associated with the process of bulk deposit formation of Tl on the Tl UPD and the magnitude of these current peaks is more negative as the scan rate decreases. In this same potential region, there is an anodic peak between −585 and −590 mV associated with the process of dissolution of bulk thallium deposition, which also depends upon the scan rate.

On other hand, the analysis of frequency variation (Δf) responses as a function of the potential explored (Fig. 2(b)) offers more information on the formation process of thallium films. For example, the frequency changes observed during the scan towards negative potentials are very small ranging between +400 and −500 mV. These changes of frequency, not visible in our responses, reach values close to 80 Hz and are associated with thallium UPD process on the electrode. It is appropriate to mention that as the potential is swept towards values more negative than −500 mV, Δf decreases (the mass increases), but this decrease is not linear, which seems to indicate that during bulk thallium deposition there are mechanical tensions resulting from the differences in atomic sizes (a_{Tl} = 1.48 Å, a_{Au} = 1.50 Å) that remain until the film thickness reaches values close to 3 kHz.

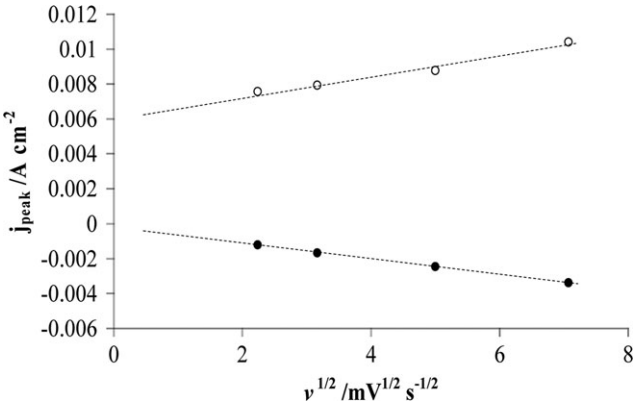

Fig. 3 Plot of the peak current densities as a function of the square root of the scan rate for cathodic (deposition) and anodic (stripping) processes in Fig. 2(a).

If the potential is scanned up to −1 V the frequency response reaches a minimum ($-\Delta f_{min}$, film thickness) that depends upon the scan rate. Thus, if the scan rate is 5 mV s^{-1}, the Δf_{min} is almost −50 kHz, whereas if the rate is 50 mV s^{-1}, the Δf_{min} is almost −5 kHz.

This behaviour is due to the fact that sweep duration is shorter at higher sweep rates, resulting in less mass of Tl deposited on the electrode.

In order to know if the thallium deposition and stripping processes are controlled by diffusion, the plot of the peak current (j_{peak}) as a function of square-root of the scan rate, v (Fig. 3) was obtained.

In accord with this figure, the behavior of the curve is linear which shows that thallium deposition and stripping processes are controlled by diffusion.[39,40]

The integration of deposition process using CV profiles gave the charge densities (ΔQ) for the range of scan rates explored, which were subsequently plotted *vs.* the respective frequency changes to obtain C_f values; however, we found that these values depended upon the thicknesses of Tl deposits (l_f). Fig. 4 shows a curve of the sensitivity constant as a function

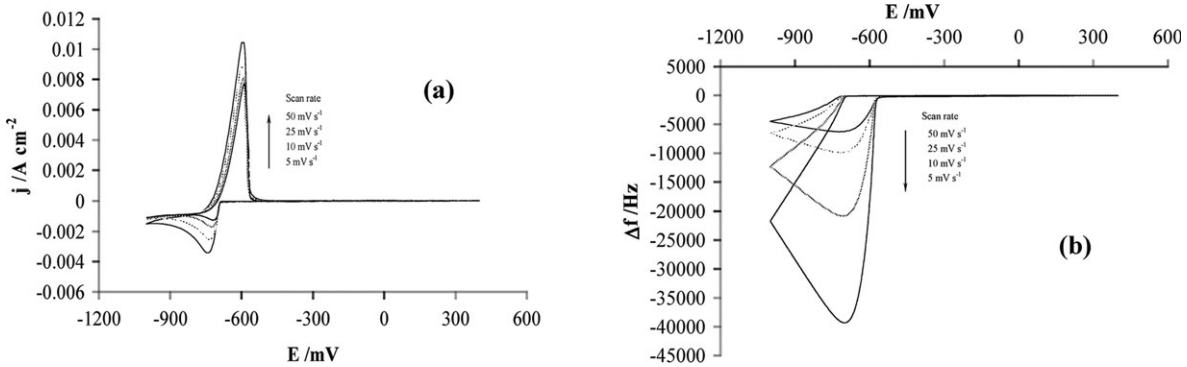

Fig. 2 (a) Series of cyclic voltammogram (CV) profiles for Tl deposition on and stripping from Au electrode in 1 M $NaClO_4$ (pH 3.5) + 1 mM Tl(I) at room temperature and different scan rates, v: 5, 10, 25, 50 mV s^{-1}; arrows indicate the changes brought about by the scan rate increase. (b) Series of quartz-crystal frequency changes (Δf) during the potential scan obtained concurrently with cyclic voltammograms (CV).

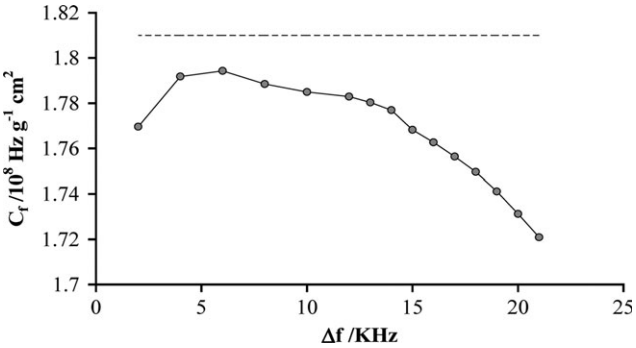

Fig. 4 Graph of the calibration constant (C_f) as a function of frequency change ($|\Delta f|$: thickness) during potential scan. Au electrode in 1 M $NaClO_4$ (pH 3.5) + 5 mM Tl(I) at room temperature at a 5 mV s^{-1} scan rate.

of film thicknesses (l_f) at 5 mV s^{-1} in order to illustrate the general behaviour of other scan rates.

$$l_f = -\frac{N\rho_q}{\rho_f f_0^2}\Delta f \qquad (12)$$

To prepare this curve we used eqn (12) which shows that l_f is proportional to $-\Delta f$ (where ρ_f is the density of the thallium and other parameters have been mentioned in expression (2)).

The plot of C_f as a function of thickness ($-\Delta f$) of the Tl deposit reveals that C_f tends to decrease from 1.791×10^8 to 1.725×10^8 g^{-1} Hz cm^2 as the thickness is increased from 8 to 21 kHz. In addition, if the deposit thickness is between 6 kHz and 3.5 kHz then the value of C_f is closer to the theoretical value (1.819×10^8 g^{-1} Hz cm^2 (5.425×10^{-9} g Hz^{-1} cm^{-2})). Finally, when the thickness of the Tl films is smaller than 3 kHz then the C_f constants obtained (1.775×10^8 g^{-1} Hz cm^2) are closer to the theoretical value.

It is important to mention that the effect of the acoustic impedance on the sensitivity constant was first considered to explain these results but the C_f values reported in this work show similar behaviours at both high and low thicknesses ($-\Delta f$) it was considered that the technique used to prepare the films directly affects their morphological properties and probably the acoustic impedance as well.

In consequence, this behaviour of C_f values is associated with the morphology of thallium films obtained using this methodology. To understand this, Fig. 5 shows a schematic representation of the different states of deposits.

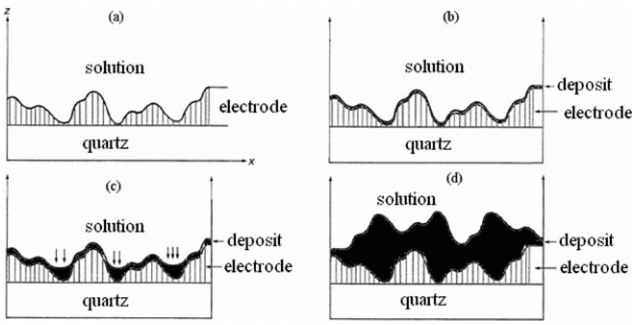

Fig. 5 Graphic representation of the clean electrode (a) and deposit formation at low (b), medium (c) and high thicknesses (d).

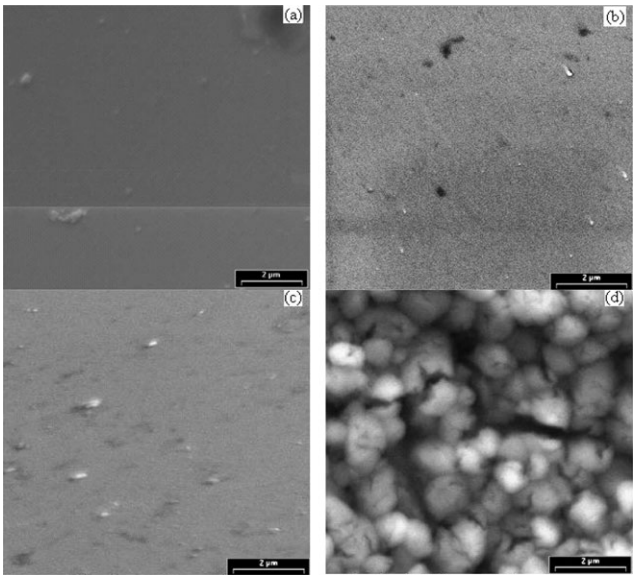

Fig. 6 Micrographs taken from: (a) deposit-free electrode and electrode with deposits of (b) 1 kHz, (c) 3 kHz and (d) 7 kHz thickness, made potentiodynamically from a solution 1 M [$NaClO_4$] + 5 mM [Tl^+], pH 3.5 at a rate of 10 mV s^{-1}.

According to this figure, thin deposits (Fig. 5(a)) reproduce the electrode morphology thus having roughness similar to that of the electrode. This makes the motion of vibrating surface of the resonator become more complicated than for a smooth surface. A variety of additional mechanisms of coupling between the acoustic waves and the motion of the liquid can arise, such as generation of nonlaminar motion, conversion of the in-plane surface motion into motion in the direction perpendicular to the surface, and trapping of liquid by cavities and pores. It has been experimentally demonstrated[41–44] that a roughness-induced shift of the resonant frequency includes both the inertial contribution, due to the mass of the liquid rigidly coupled to the surface, and the contribution due to the additional viscous energy dissipation caused by the nonlaminar motion in the liquid. In this case, these processes can contribute to the overestimation of the values of the sensitivity constant.

However, the continued growth of the deposit is believed to make the deposit reach such a thickness (approximately between −2 and −5 kHz, Fig. 5(b) and (c)) that the electrode roughness disappears, so the thallium film obtained is smooth and shiny, and thereby the changes of frequency (Δf) are directly related to mass changes. In this situation the C_f values obtained are very similar to theoretical value.

Finally, if the thickness of thallium deposit is even more increased, the metallic film changes from smooth to even rougher, Fig. 5(d), and consequently the same situation occurs as at low thicknesses.

To check the validity of these hypotheses, we proceeded to obtain photos of the deposits in the three situations posed above (Fig. 6) using just one of the scan rates at which the possible relationship between C_f and morphologic properties is best observed.

Fig. 6 shows the images of the three types of deposits obtained by scanning electron microscopy at the same scale using a scan rate of 10 mV s^{-1}.

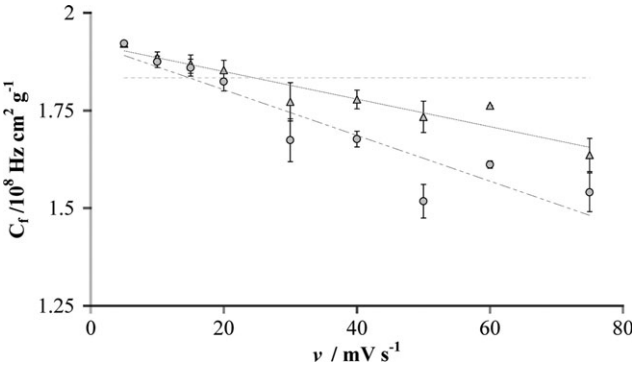

Fig. 7 Plots of sensitivity constant C_f as a function of scan rate (v) at the thickness of 3.5 kHz (○) and 4.5 kHz (△).

Fig. 6(a) shows the image of deposit-free gold electrode with a smooth and shiny surface. On the other hand, the image from Fig. 6(b), corresponding to thallium deposit of 1 kHz thickness, shows the film with practically the same characteristics as that on the gold electrode, with the only difference consisting in small, randomly distributed accumulations of thallium. If the thickness is greater than 3 kHz, the morphology of thallium deposit is well observed to evolve to a very rough structure (Fig. 6(c) and (d)).

These results confirm the hypotheses posed about the effect of roughness on the value of C_f.

On the basis of these results, sensitivity constants were calculated using the zone of maximum C_f–Δf curves at different scan rates.

Fig. 7 shows the plot of C_f *vs.* scan rate for Tl deposit thicknesses of 3.5 and 4.5 kHz. As may be observed, for both thicknesses used, the C_f values follow a linear behavior with the speed of scanning.

A careful analysis of these curves reveals that the values of C_f can be grouped in two series according to the rate of scanning: the first series includes scanning speeds ranging between 5 and 20 mV s^{-1} and the second series comprises speeds between 20 and 75 mV s^{-1}. In the first series, C_f values are between 1.824×10^8 g^{-1} Hz cm^2 and 1.921×10^8 g^{-1} Hz cm^2, which implies that these values differ from the theoretical value by -0.36 to $+4.72\%$ (relative error (%) = 100 [C_f(experimental) − C_f(theoretical)]/C_f(theoretical)). In the case of the second series, these values fall between 1.772×10^8 and 1.636×10^8 g^{-1} Hz cm^2, so they differ from the theoretical value by -1.47 up to -12.42%.

We assume that this behavior of C_f as a function of scan rate (v) is due to the fact that at high values of v the deposit is no longer uniform and consequently, the Sauerbrey expression is not valid. This result implies that the values of C_f have to be obtained at Δf (thickness) restricted between 4.5 to 3.5 kHz. Table 1 shows the C_f obtained at 3.5 kHz.

A careful analysis of results reveals that the calibration constant is very close to the theoretical when the scan rate is between 5 and 20 mV s^{-1}. The average value of C_f is 1.882×108 g^{-1} Hz cm^2 which differs by $+2.6\%$ from the theoretical value.

3.2.2 Potentiostatic method. In this series of experiments, the potential is stepped from an initial value E_i where no Tl is reduced on the electrode to the final one (E_f) between -780 and -980 mV with a potential interval (ΔE) of 20 mV; the step duration (Δt) is 120 s. This experimental potential range was selected from CV data (see Fig. 2(a)). Plots of C_f as a function of thickness (Δf) of the electrodeposited Tl layer, obtained in the selected potential range, are shown in Fig. 8.

Table 1 Calibration constant (C_f) data as a function of scan rate (v) at a thickness of 3.5 kHz. SD is standard deviation

v/mV s^{-1}	$C_f/10^8$ Hz cm^2 g^{-1}	Relative error (%)	SD
5	1.9210	+4.75	0.0039
10	1.8851	+2.11	0.0143
15	1.8687	+0.76	0.0236
20	1.8535	+2.04	0.0251
30	1.7722	−1.47	0.0490
40	1.7781	−2.12	0.0239
50	1.7337	−3.91	0.0402
60	1.7626	−3.88	0.0001
75	1.6360	−12.42	0.0425

A careful analysis of these plots indicates that all curves have the same behavior: C_f is close to the theoretical value when the thickness is between 2 and 6 kHz, provided that the E_f is between -720 and -900 mV. In addition, if the thickness is greater than 6 kHz, the C_f values are almost constant and close to the theoretical value when the E_f is -720 and -880 mV, but farther from the theoretical value when the E_f is more negative than -880 mV.

Fig. 9 shows the C_f plot as a function of E_f at different thicknesses (Δf). The resulting curves confirm the statement in the above paragraph but allows us to obtain further data. For example, when the thickness is only 2 kHz, the C_f determined between -720 and -900 mV is almost $+10\%$ different from the theoretical value; whereas for potentials more negative than -900 mV, the C_f difference is almost $+30\%$.

On the other hand, if the thickness is 4 kHz, the relative error of C_f falls between -2 and -7% with respect to the theoretical value when the E_f of the deposit is restricted between -720 and -840 mV. Additionally, with deposits of the same order of thicknesses, if the potentials are more negative than -840 mV, the C_f has a tendency to increase the relative error from -7% to almost -60%.

This figure also shows that a behavior limit in the curves is reached at thicknesses greater than 6 kHz. If the deposit

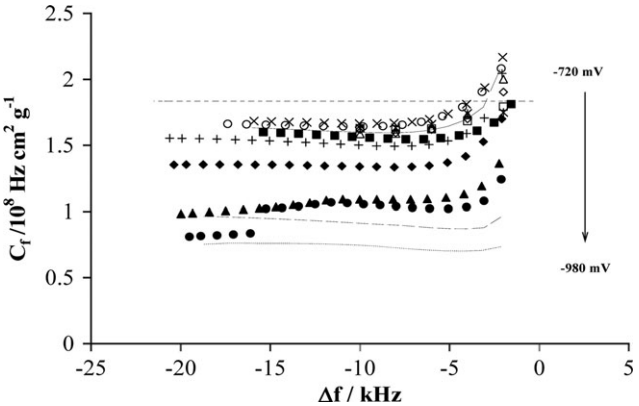

Fig. 8 Plots of calibration constant, C_f, as a function of thickness (Δf) of Tl deposit for different values of potential E_f.

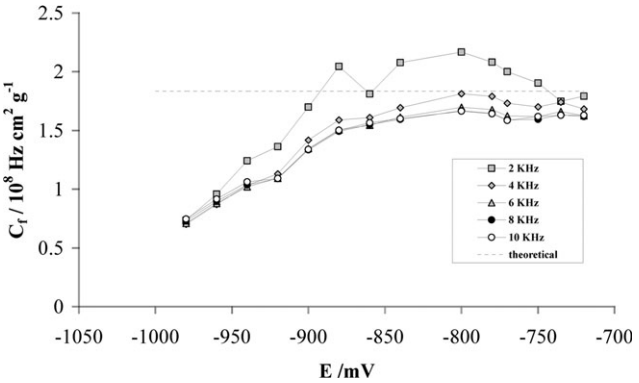

Fig. 9 Curves of sensitivity constant C_f as a function of the potential applied to different deposit thicknesses ($-\Delta f$).

thickness (Δf) is 6 kHz, the C_f has errors of -7% at E_f values falling between -720 and -840 mV. For potentials more negative than -840 mV, the error in the C_f can vary from -15 to -60%.

C_f values as a function of potential stepped at thicknesses between 4 and 6 kHz are shown in Fig. 10 and Table 2.

The C_f values in this curve present different tendencies based on the potential zone in which E_f is localized. When the E_f potential is nearer to the potential in which the fall of current in voltammogram takes place (see Fig. 2(a)), then C_f approaches the theoretical value; whereas if the E_f is more negative than $E_{j=0}$, the value of C_f moves away from its theoretical value.

The values of C_f fall between 1.694×10^8 and 1.812×10^8 g^{-1} Hz cm^2, which is equivalent to having errors between -1 and -7.6% with respect to the theoretical value, when E_f is between -700 and -840 mV. On the other hand, C_f is lower than 1.609×10^8 g^{-1} Hz cm^2 when E_f is more negative than -840 mV.

Since the thickness is practically the same for all deposits, the C_f behavior is a consequence of the fact that the current flowing at potentials more negative than -840 mV is a result of two processes: reduction of Tl^+ ion and of H^+ ion. This can be better seen in Fig. 11 when $[Tl^+] = 10$ mM, where the current obtained from the mass is compared using the best C_f (Fig. 11(b)). The j_m current is practically the same for potentials more positive than -840 mV; on the contrary, the

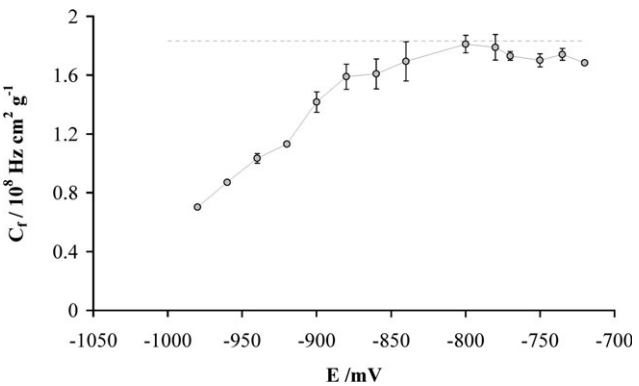

Fig. 10 Plot of C_f values as a function of potential stepped at the thickness of 4 kHz.

Table 2 Calibration constant data as a function of potential stepped (E_f) with the thickness ranging between 4 kHz and 6 kHz

E_f/mV	$C_f/10^8$ Hz cm^2 g^{-1}	Relative error (%)	SD
−1000	1.4259	22.246	0.0045
−980	0.7016	61.741	0.0132
−960	0.8706	52.529	0.0330
−940	1.0337	43.635	0.0114
−920	1.1307	38.344	0.0689
−900	1.4170	22.732	0.0859
−880	1.5897	13.312	0.1020
−860	1.6089	12.267	0.1328
−840	1.6943	7.608	0.0592
−800	1.8119	1.195	0.0869
−780	1.7900	2.391	0.0299
−770	1.7312	5.596	0.0444
−750	1.7008	7.252	0.0402
−735	1.7416	5.029	0.0322

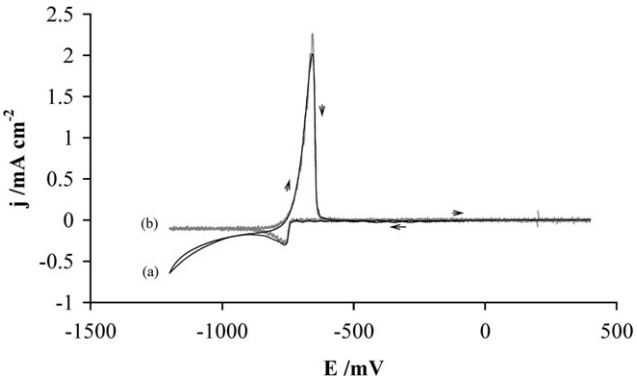

Fig. 11 Voltammetric responses for processes of thallium deposit formation and dissolution on gold electrode. (a) Voltammogram obtained concurrently with mass response, (b) voltammogram obtained from mass response: $[Tl^+] = 1$ mM, pH = 3.5 and $v = 5$ mV s^{-1}.

j_m is lower in the curve b than in the curve a for potentials more negative than -840 mV, which indicates that another process is taking place simultaneously with the reduction of thallium ion.

3.2.3 Galvanostatic method. This method is the simplest of the three because the films are formed by applying a constant current to the electrode during a determined time period. Nevertheless, one cannot apply just any value of the current because it affects the morphology of the formed deposits. For example, some authors[45,46] have found that if the current imposed is higher than the limiting value (I_{lim}), the film can grow dendritically and the deposit is not uniform. On the contrary, if a lower current than I_{lim} is applied then the deposit can be compact and shiny. The reason for this is that I_{lim} expresses the limit condition between the charge transfer and the mass transfer steps which restrict deposit formation processes. This information allowed us to set up a methodology to determine a suitable current that is to be used from the I_{lim} value prior to obtaining C_f. This parameter can be determined by voltammetry in the following manner: the value of the apparent limit current (I_{lim}) was obtained from the part of the voltammogram related to the process of deposit formation (see Fig. 2(a)) at different scan rates. These values were used to

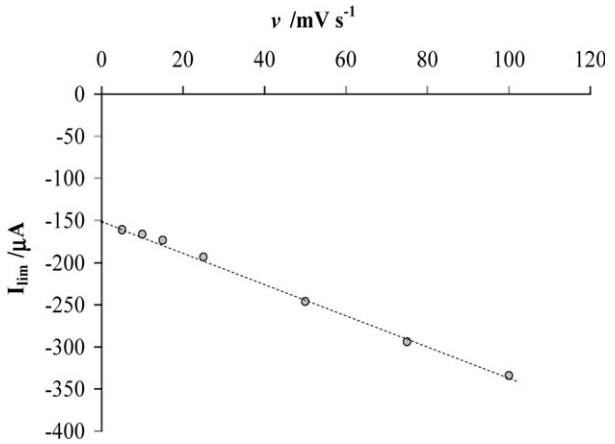

Fig. 12 Plot of the apparent limit current (I_{lim}) at different scan rates (v) during the deposition process of thallium onto gold electrode by cyclic voltammetry.

prepare a plot of apparent I_{lim} as a function of scan rate, so the I_{lim} was obtained by extrapolation when $v \rightarrow 0$. Fig. 12 shows the curve obtained for a Tl concentration of 5 mM.

As may be seen, the behavior of I_{lim} is linear in the range of speeds explored, and extrapolation generates a value of I_{lim} of 150 mA. From this value it was decided to use different currents that were fractions of I_{lim} between 80 and 100%. The determination of the sensitivity constant is simple as the charge is obtained using the following expression

$$\Delta Q = I_{appl} t_{step} / A \qquad (13)$$

where I_{appl} is the current applied during the determined time interval, t_{step} and A is the area of the electrode. The plot of C_f as a function of the deposit thickness (Δf) is shown in Fig. 13. As is obvious for all the curves, the value of C_f depends on the thickness of the deposit (Δf) when Δf is greater than 6 kHz. Additionally it is observed that between 0 and 6 kHz, curves display the same behavior regardless of the value of I_{appl}. On the other hand when the deposit thicknesses are greater than 6 kHz, the C_f differs more from the theoretical value if I_{appl} is closer to I_{lim}.

It is important to mention the surprising superposition of the curves obtained when the currents applied fall between 95 and 98% of I_{lim} for the entire range of thicknesses (Δf), which

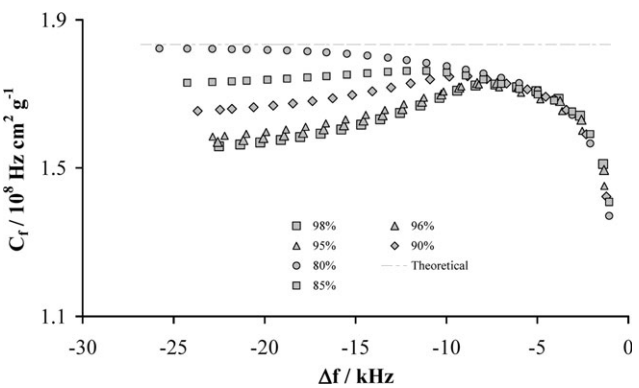

Fig. 13 Plots of the sensitivity constant (C_f) as a function of thickness (Δf) during the deposition process of thallium onto gold.

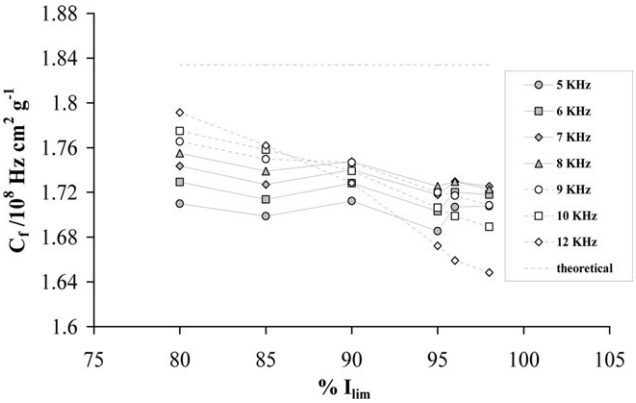

Fig. 14 Plots of the sensitivity constant (C_f) as a function of the current applied (%I_{lim}) during the deposition process of thallium onto gold.

implies that a limit situation is reached using this method. Additional information can be obtained if the C_f values are plotted as a function of imposed current (%I_{lim}), Fig. 14 and Table 3.

It should be noted that experimental values of C_f are farther from the theoretical value when the stepped current is between 90 and 98% of I_{lim} if the thickness is between 5 and 12 kHz. In this current range the error is between +6 and +9.8%. On the contrary, when the stepped current is between 80 and 85% of I_{lim} for this same thickness range, then C_f can attain its maximum value with respect to the theoretical value. In this case the difference from the theoretical value is just +2.2% (thickness 12 kHz).

As mentioned above, the current imposed to prepare the deposits of thallium affects their morphologic characteristics in such a way that the closer I_{appl} is to I_{lim} the less uniform and rigid is the film, and in consequence, the restrictions to employ the Sauerbrey expression are not applicable. On the contrary, the farther is I_{appl} from I_{lim} the film is more uniform and rigid and in consequence, the restrictions to employ the Sauerbrey's expression are appropriate.

Table 3 shows data of C_f, when I_{appl} is between 80 and 85% at a thickness ranging between 5 and 14.5 kHz. From the corresponding data in the table, C_f falls between 1.743×10^8 g^{-1} Hz cm^2 (I_{appl} = 80%I_{lim} and Δf = 7 kHz) and 1.727×10^8 g^{-1} Hz cm^2 (I_{appl} = 85%I_{lim} and Δf = 7 kHz), which represents errors of almost +5%. This value is in good agreement with the C_f value that would be determined using a silver deposit with the resulting errors falling between 2% and 25%.[11]

3.2.4. Comparison of C_f values obtained using the three methods. The process of sensitivity constant determination using the three methods yields similar values of C_f which are seen to be affected by the same factors. In the case of cyclic voltammetry, the values fall within a range of 1.824×10^8 and 1.921×10^8 g^{-1} Hz cm^2, at a thickness of 3.5 kHz. These values exhibit a strong dependence on the scan rate, however extrapolation of the C_f *versus* scan rate in relation to the zero scan rate yields a value of 1.921×10^8 g^{-1} Hz cm^2 at a scan rate between 5 and 20 mV s^{-1}, which is close to the theoretical value by +4.7%. On the contrary when the average value of C_f is obtained in the entire

Table 3 Calibration constant data as a function of the current applied when the thickness is between 8 and 10 kHz

	$80\%I_{lim}$			$85\%I_{lim}$		
Δf/kHz	C_f[a]	Relative error[b] (%)	SD	C_f[a]	Relative error[b] (%)	SD
5	1.7099	6.7591	0.0194	1.6987	7.3703	0.0125
6	1.7292	5.7065	0.0135	1.7137	6.5533	0.0073
7	1.7435	4.9271	0.0079	1.7271	5.8212	0.0046
8	1.7550	4.2985	0.0039	1.7390	5.1731	0.0020
9	1.7655	3.7274	0.0010	1.7498	4.5826	0.0008
10	1.7748	3.2187	0.0026	1.7581	4.1282	0.0004
12	1.7914	2.3159	0.0064	1.7620	3.9191	0.0002
14.5	1.8035	1.6546	0.00755	1.7560	4.2472	0.0004

[a] $C_f/10^8$ g^{-1} Hz cm^2. [b] Relative error (%) = $100[C_f(\text{experimental}) - C_f(\text{theoretical})]/C_f(\text{theoretical})$.

range of scan rate (1.882×10^8 g^{-1} Hz cm^2), it only differs by +2.6% with regard to the theoretical value.

The values of C_f obtained by chronoamperometry fall between 1.694×10^8 and 1.811×10^8 g^{-1} Hz cm^2 at a thickness between 4 and 6 kHz when the potential range is between −700 and −840 mV. These values differ by −1 to +5% from the theoretical value.

In the case of C_f values obtained by chronopotentiometry, they show dependence on the stepped current since C_f is farther from the theoretical value as the current imposed approaches the limit current. In addition, the C_f values obtained using this method approach the theoretical value at greater thicknesses than those obtained by the two other methods, which seems to demonstrate that Saurbrey's equation is appropriate for these deposits since they are more uniform and rigid. The C_f values of 1.743×10^8 and 1.791×10^8 g^{-1} Hz cm^2 are determined at the current stepped between 80 and 85% of the limit current when the thickness ranges between 7 and 14 kHz.

It is important to mention that the effect of the acoustic impedance[47] on the sensitivity constant was first considered to explain these results but a more careful analysis showed that this effect would be important only if the C_f had the same behaviour in the same range of $-\Delta f$ (thickness). Since this is not the case and because different behaviours of C_f fall within different ranges of Δf, in accordance with the technique of deposit preparation used, this effect was ruled out.

In addition, because the C_f values reported in this work show similar behaviours at both high and low thicknesses ($-\Delta f$) it was considered that the technique used to prepare the films directly affects their morphological proprieties and probably the acoustic impedance as well. This hypothesis is supported by our images.

In consequence, these behaviours of C_f values are associated with the morphology of thallium films obtained using these methodologies.

3.3 Surface state of used electrodes

We obtained a voltammogram of the electrodes used in this determination of C_f in an acid solution of H_2SO_4 to check the state of their surface after experiments. Two typical CV of the same Au electrode used in this work before and after experiments are shown in Fig. 15.

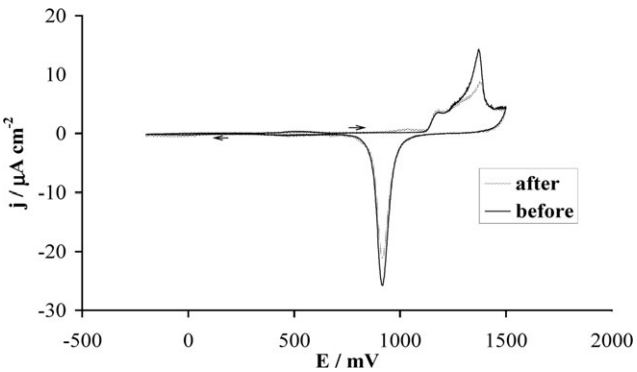

Fig. 15 Two typical CVs of the same Au electrode used in this work obtained before and after experiments in a solution of 0.1 M H_2SO_4at 50 mV s^{-1}.

A careful analysis of these responses shows that there are no significant differences between the two experimental situations. Only the height of oxidation peak at +1376 mV decreases, but this behavior is typical of a used electrode.

These characteristics of CVs reveal that the determination of C_f with thallium has no important effect on the surface state of the electrodes and they can be used in subsequent experiments.

4. Conclusions

The results obtained from the determination of C_f by the three study techniques using thallium deposits showed a significant dependence of C_f on the film thickness.

This dependence consist in the fact that at low thicknesses the C_f values obtained are farther from the theoretical value because the thallium film reproduces the substrate's morphology and therefore, a microroughness effect must be considered to explain this effect. At intermediate thicknesses, the deposit is smoother and the C_f constants approach the theoretical value, which reveals no influence of roughness on these films.

On the other hand, if thallium films are very thick, the C_f values move away from the theoretical value due to their microroughness.

On comparing the methodologies for obtaining films, the results achieved showed that cyclic voltammetry generates the C_f values closer to the theoretical one when the scan rate is

lower than 30 mV s^{-1}. When C_f is obtained at constant potential, the results attained showed that the best values are achieved between −710 and −680 mV. Lastly, if C_f is obtained at constant current, the nearest data have relative errors below 7% at the current ranging between 80 and 85% of I_{lim}.

Finally, the voltammograms of the electrodes used in sulfuric acid before and after obtaining C_f show no significant differences, so the calibration process does not affect surface properties of the electrodes and these can therefore be reused in further experiments.

Acknowledgements

This research was performed under the auspices of the Universidad Autonoma de San Luis Potosí through the Teaching Support Fund and the Ministry of Public Education through the Program for Teachers' Improvement (PROMEP). A. L. D. M. is grateful for the financial aid granted by CONACYT for her master studies.

References

1 K. Leistner, A. Krause, S. Fahler, H. Schlorb and L. Schultz, *Electrochim. Acta*, 2006, **52**, 170.
2 K. Ogura, K. Nakaoka and M. Nakayama, *J. Electroanal. Chem.*, 2000, **486**, 119.
3 A. G. C. Márquez, L. M. T. Rodríguez and A. Montes-Rojas, *Electrochim. Acta*, 2007, **52**, 5294.
4 J. Lidera, M. Skompska and K. Jackowska, *Electrochim. Acta*, 2001, **46**, 4125.
5 P. Kern and D. Landolt, *J. Electrochem. Soc.*, 2000, **147**, 318.
6 S. Langerock and L. Heerman, *J. Electrochem. Soc.*, 2004, **151**, C155.
7 A. Montes-Rojas, C. Nieto-Delagdo and L. M. Torres-Rodríguez, *New J. Chem.*, 2007, **31**, 1769.
8 F. N. Nunalee, K. R. Shull, B. P. Lee and P. B. Messersmith, *Anal. Chem.*, 2006, **78**, 1158.
9 W. Visscher, J. F. E. Gootzen, A. P. Cox and J. A. R. van Veen, *Electrochim. Acta*, 1997, **43**, 533.
10 A. Montes-Rojas and E. Chainet, *J. Mex. Chem. Soc.*, 2005, **49**, 336.
11 A. Zolfaghari, B. E. Conway and G. Jerkiewicz, *Electrochim. Acta*, 2002, **47**, 1173.
12 C. H. de Long, J. J. Donohue and D. A. Buttry, *Langmuir*, 1991, **7**, 2196.
13 G. A. Snook, A. M. Bond and S. Fletcher, *J. Electroanal. Chem.*, 2002, **526**, 1.
14 N. Lebbad, J. Voiron, B. Nguyen and E. Chainet, *Thin Solid Films*, 1996, **275**, 216.
15 D. A. Buttry and M. D. Ward, *Chem. Rev.*, 1992, **92**, 1355.
16 M. Hepel, in *Interfacial Electrochemistry, Theory Experiment and Applications*, ed. A. Wieckowski, Marcel Dekker, New York, 1999, ch. 34.
17 G. Sauerbrey, *Z. Phys.*, 1959, **155**, 206.
18 A. Arnau, *Sensors*, 2008, **8**, 370.
19 S. Bruckeinstein and S. Swathirajam, *Electrochim. Acta*, 1985, **30**, 851.
20 C. Gabrielli, M. Keddam and R. Torresi, *J. Electrochem. Soc.*, 1991, **138**, 2657.
21 G. Vatankhah, J. Lessard, G. Jerkiewicz, A. Zolfaghari and B. E. Conway, *Electrochim. Acta*, 2003, **48**, 1613.
22 D. M. Soares, *Meas. Sci. Technol.*, 1993, **4**, 549.
23 A. Montes-Rojas, These de Docteur, Université Joseph Fourier-Grenoble 1, France, 2000, ch. 3.
24 E. Gileadi and V. Tsionsky, *J. Electrochem. Soc.*, 2000, **147**, 567.
25 G. G. Lang, M. Ujvári and G. Horányi, *J. Electroanal. Chem.*, 2002, **522**, 179.
26 D. A. Buttry, in *Applications of the Quartz Crystal Microbalance to Electrochemistry*, ed. A. J. Bard, Marcel Dekker, New York, 1991, vol. 17, p. 1.
27 G. Ningyu and D. Shaojun, *Electrochem. Commun.*, 2000, **2**, 713.
28 Z. Shi, S. Wu and J. Lipkowski, *J. Electroanal. Chem.*, 1995, **384**, 171.
29 E. Schmidt and S. Stucki, *J. Electroanal. Chem.*, 1972, **39**, 63.
30 S. G. Garcia, D. Salinas, C. Mayer, J. R. Vilche, H.-J. Pauling, S. Vinzelberg, G. Staikov and W. Lorenz, *Surf. Sci.*, 1994, **316**, 143.
31 Y. Ratieuville, P. Viers, J. Alexandre and G. Durand, *Electrochem. Commun.*, 2000, **2**, 839.
32 K. Uosaki, S. Ye, Y. Oda, T. Haba and K. Hamada, *Langmuir*, 1997, **13**, 594.
33 A. Hamelin, A. Katayama, G. Picq and P. Vennereau, *J. Electroanal. Chem.*, 1980, **113**, 293.
34 W. R. Heineman, in *Laboratory Techniques in Electroanalytical Chemistry*, ed. P. T. Kissinger and W. R. Heineman, Marcel Dekker, New York, 1996, ch. 3, p. 59.
35 M. Pourbaix, in *Atlas d'quilibres Electrochimiques á 25 °C*, ed. Gautier-Villars & Cie, Paris, 1963, p. 414.
36 H. Angerstein-Kozlowska, B. E. Conway, B. Barnett and J. Mozota, *J. Electroanal. Chem.*, 1979, **100**, 417.
37 A. Montes-Rojas and E. Chainet, *J. Chil. Chem. Soc.*, 2007, **52**, 1099.
38 R. R. Adzic, J. Wang and B. M. Ocko, *Electrochim. Acta*, 1995, **40**, 83.
39 S. Srinivasan and E. Gileadi, *Electrochim. Acta*, 1966, **321**, 11.
40 V. A. Vincent and S. Bruckenstein, *Anal. Chem.*, 1973, **45**, 2036.
41 Z. Lin and M. D. Ward, *Anal. Chem.*, 1995, **67**, 685.
42 L. Daikhin, E. Gileadi, G. Katz, V. Tsionsky, M. Urbakh and D. Zagidulin, *Anal. Chem.*, 2002, **74**, 554.
43 S. Wehner, K. Wondraczek, D. Johannsmann and A. Bund, *Langmuir*, 2004, **20**, 2356.
44 I. Efimov, R. Hillman and J. W. Schultze, *Electrochim. Acta*, 2006, **51**, 2572.
45 R. Winand, *J. Phys. IV*, 1994, **4**, C1–55.
46 R. Winand, *J. Appl. Electrochem.*, 1991, **21**, 25.
47 C.-S. Lu and O. Lewis, *J. Appl. Phys.*, 1972, **43**, 4385.

